Biochimica et Biophysica Acta 814 (1985) 289–299
Elsevier

BBA 72521

Cell age-dependent changes in deformability and calcium accumulation of human erythrocytes

Takeshi Shiga, Misuzu Sekiya, Nobuji Maeda, Kazunori Kon and Masaharu Okazaki

Department of Physiology, School of Medicine, Ehime University, Shigenobu, Onsen-gun, Ehime 791-02 (Japan)

(Received September 7th, 1984)
(Revised manuscript received December 18th, 1984)

Key words: Cell deformability; Ca^{2+} transport; Aging; Energy charge; Membrane fluidity; (Erythrocyte membrane)

The deformability of human erythrocytes was measured in a rheoscope, as a function of intracellular calcium content (varied with ionophore (A23187) and $CaCl_2$) without complete ATP depletion and echinocytic transformation. (1) Loading calcium into intact erythrocytes (calcium content: 16.8 μmol/l packed cells = 1.48 amol per cell), the cell volume and energy charge gradually decreased. Further, the membrane fluidity of the lipid portion decreased without crosslinking of membrane proteins. (2) A distinct transition from deformable to undeformable cells was observed by the rheoscope technique: i.e., 50% transition occurred at 40–50 μmol calcium/l packed cells (= 3.5–4.0 amol per cell) and more than 90% above 100 μmol/l packed cells (= 6.5 amol per cell) at a shear stress of 140 dyn/cm². The deformable cells maintained their deformability to ellipsoidal disks independent of the average calcium content. (3) The undeformable cells, separated as high-density cells by density gradient centrifugation after calcium-loading, showed lower glucose-6-phosphate dehydrogenase activity than low-density-deformable cells; thus, the calcium-loaded, undeformable cells were presumably in vivo aged cells. (4) The younger cells, fractionated as low-density cells from intact erythrocytes, were more deformable than aged cells. Upon calcium-loading, the younger cells restored their cell volume and deformability, while the aged cells, containing originally more calcium and less ATP, decreased their volume and became undeformable. Therefore, calcium accumulation by ionophore-$CaCl_2$ takes place in preference to aged cells of lower energy metabolism, and leads to cellular dehydration and loss of deformability, due to condensed hemoglobin and altered membrane organization.

Introduction

The contribution of intracellular calcium to the deformability and life-span of erythrocytes has been suggested in an earlier study [1]. It is known that calcium-loading with ionophore (e.g., A23187) reduces cell volume, decreases deformability and, further, induces echinocytosis [2–4]. Since the cellular deformability is influenced by many factors [5], it is necessary to investigate the relationship between calcium content, energy metabolism and deformability. The erythrocytes possess a Ca^{2+}-pump to extrude the incoming Ca^{2+} at the cost of ATP [6,7], maintaining an intracellular calcium level as low as 15–18 μmol/l packed cells [8]. The calcium content is controlled by the Ca^{2+}-ATPase

Abbreviations: Hepes, 4-(2-hydroxyethyl)-1-piperazineethanesulfonic acid; DMSO, dimethylsulfoxide; SDS, sodium dodecylsulfate; glucose-6-phosphate dehydrogenase, D-glucose-6-phosphate: NADP 1-oxidoreductase; $[Hb]_i$, mean cell hemoglobin concentration.

activity, which is regulated by calmodulin and other proteins, by phospholipids and by Mg^{2+} and ATP levels [7]. Therefore, the ability for Ca^{2+} extrusion, against calcium-loading with ionophore and $CaCl_2$, must be related to energy metabolism or to in vivo aging of individual erythrocytes.

Having these complexities in mind, we have examined the changes in cellular deformability by means of a high-shear rheoscope [9,10] as a function of intracellular calcium content. For this purpose, appropriate calcium-loading with A23187 and $CaCl_2$ of intact erythrocytes (up to several times the normal level) was carried out, avoiding complete ATP depletion and echinocytic transformation.

We observed a distinct transition from the deformable to the undeformable state of the erythrocytes induced by calcium-loading in the range of intracellular calcium, 30–100 μmol/l packed cells. Simultaneously, various determinant factors of deformability as well as some cell age-related factors were monitored, i.e., cell shape, hemoglobin concentration, lipid membrane fluidity, crosslinking of membrane proteins, glucose-6-phosphate dehydrogenase activity, ATP and 2,3-diphosphoglycerate levels, etc. We found that calcium accumulation preferably took place in erythrocytes of low energy metabolism, presumably in vivo aged cells, and that calcium-overloaded cells became undeformable.

This paper describes such distinct change in cellular deformability, as well as decreased cell volume and energy charge, as a function of intracellular calcium level when varied with ionophore A23187 and $CaCl_2$. The following phenomena will be shown: (i) an overall relationship between total calcium content and deformability, cell volume and hemoglobin concentration; (ii) a relationship between calcium accumulation and decline of energy charge; (iii) a change of membrane fluidity induced by calcium-loading; and (iv) cell age-dependent calcium accumulation and loss of deformability. The possible roles of intracellular calcium for regulation of deformability will be discussed.

Materials and Methods

Human erythrocytes and calcium-loading procedure. The erythrocytes were collected from fresh heparinized venous blood, discarding plasma and buffy coat after centrifugation (3000 rpm, 10 min, at 4°C). The erythrocytes were washed three times with isotonic Hepes-saline solution (123 mM NaCl/5 mM KCl/50 mM Na-Hepes buffer/5.6 mM glucose (pH 7.4), 285 mosM). The erythrocytes were incubated with ionophore A23187 (purchased from Calbiochem., San Diego, CA., U.S.A., dissolved in ethanol/DMSO (3 : 1, v/v) before use) and $CaCl_2$ in the Hepes-saline solution at a hematocrit of 20% for 40 min at 37°C. In most cases, 1.5 μM A23187 and 2–20 μM $CaCl_2$ were added in the incubation medium, as to obtain final intracellular calcium content of 30–100 μmol/l packed cells, avoiding considerable loss of ATP and echinocytosis. After incubation, the erythrocytes were washed once with isotonic saline solution containing 0.5 g/dl human albumin (fatty acid free, fraction V, Miles Lab., Elkhart, IN, U.S.A.) to remove ionophore A23187, then washed four times with 20 vol. of isotonic NaCl solution (285 mosM; inevitably containing 0.12–0.18 μM calcium).

Cell fractionation. The density gradient centrifugation with Percoll (Pharmacia, Uppsala, Sweden) was carried out at 10000 rpm for 20 min at 20°C using an angle rotor [11]. The high-density cells (10–20% of total) sedimented in the lower half of centrifuge tube containing an appropriate concentration of isotonic Percoll solution. The low-density cells (10–20% of total) were collected from the upper half of another centrifuge tube containing a lower concentration of Percoll. The fractionated cells were washed three times with isotonic saline solution. The fractional percentage was calculated on the basis of hemoglobin concentration.

Hematological indices. The hematocrit was determined by a microhematocrit centrifuge (Kubota Manuf. Co., Model KH-120, Tokyo, Japan), hemoglobin concentration by the CN-methemoglobin method [12] and the number of cells by an automatic counter (Toa Electronic Co., Model CC-110, Tokyo, Japan); mean cell volume and mean cell hemoglobin concentration were then calculated.

Observation of cell shape. After fixation with glutaraldehyde, the cell shape was observed either under a microscope (Olympus Optics, Model BH,

Tokyo, Japan) or by a scanning electron microscope (Hitachi Manuf. Co., Model S-500, Hitachi, Japan).

Measurement of osmolarity. The freezing point of all solutions was measured by a Halbmikro osmometer (Knauer, Type M, F.R.G.), then converted to osmolarity.

Determination of intracellular calcium content. The washed erythrocytes were packed by centrifugation (final hematocrit, 75–83%). An aliquot of concentrated erythrocytes was poured into 20 vol. of 0.1 M HNO_3 with stirring and left standing for 60 min at 25°C. After centrifugation (15000 rpm, for 30 min), the supernatant was diluted (10-times) with 0.1 M HNO_3 and applied to a flameless atomic absorption spectrometer (Shimadzu Manuf. Co., Model AA-646, Kyoto, Japan) operated at 422.7 nm, with or without adding standard calcium (the final amount of calcium for the standard dilution method was 0–100 ppb). The heating of the graphite atomizer was programmed as follows: (i) drying in ramp mode (20–80°C) for 15 s, (ii) drying in ramp mode (80–120°C) for 10 s, (iii) ashing in ramp mode (120–700°C) for 15 s, (iv) ashing in step mode (1200°C for 15 s), and finally (v) atomized at 2400°C for 6 s. The amount of intracellular calcium, $[Ca]_i$, was expressed in dual units, μmol/l packed cells and amol/cell, since the cell volume changes with calcium content. The average value of a donor, incubated without ionophore A23187 and $CaCl_2$ and washed (denoted as 'calcium-unloaded erythrocytes', throughout), was 16.8 ± 2.4 (S.D.) μmol/l packed cells or 1.48 ± 0.22 amol/cell ($n = 8$), which agreed with reported values [8].

Measurement of deformability. A rheoscope [9,10,13] consisting of an inverted microscope (Olympus Optics Co., Model IMT, Tokyo Japan), a transparent 0.8° cone-plate viscometer (Tokyo Keiki Co., Model B, Tokyo, Japan) and a flashlight (Sugawara Manuf. Co., Model MS-230, Tokyo, Japan) was used; the flash photographs were taken using Kodak Tri-X film. The erythrocytes were suspended in 20% (w/v) Dextran T-40 (Pharmacia, dissolved in Hepes-saline solution (pH 7.4), 285 mosM; viscosity 18.6 cP at 25°C) and rotated at shear rates of 19–750 s^{-1} at 25°C. The biconcave disk-shaped erythrocytes were deformed to ellipsoidal disk at high shear rate and the ratio of short radius/long radius was adopted as a measure of deformation [10,13]. The distinction of deformable and undeformable cells was made at shear rates, 75 and 750 s^{-1} (= shear stress of 14 and 140 dyn/cm^2).

Measurement of membrane properties. For detecting the changes of membrane fluidity in lipid portion, the spin label method with 2-(10-carboxydecyl)-2-hexyl- and 2-(14-carboxytetradecyl)-2-ethyl-4,4-dimethyl-3-oxazolidinyloxyl (abbreviated as 12-SAL and 16-SAL, respectively: purchased from Syva Co., Palo Alto, CA, U.S.A.) was adopted, using a Varian E-3 EPR spectrometer (Palo Alto, CA, U.S.A.) as described elsewhere [14]. For detection of cross-linking of membrane proteins, SDS-polyacrylamide gel electrophoresis was carried out [10,15].

Determination of energy metabolism and enzyme activity. The amounts of ATP, ADP and AMP were determined by a liquid chromatography (Shimadzu Manuf. Co., Model LC-3A, Kyoto, Japan) with Permaphase AAX (2.1 mm × 100 cm) column, as described elsewhere [16]. The energy charge (EC) was calculated by the equation:

$$EC = (2[ATP]+[ADP])/2([ATP]+[ADP]+[AMP]).$$

The amount of 2,3-diphosphoglycerate was determined as described elsewhere [17]. Glucose-6-phosphate dehydrogenase activity was measured using a test kit (purchased from Boehringer-Mannheim, F.R.G.; Cat. No. 124672) [18].

Results

Overall relation between calcium content, deformability and cell volume

The biconcave disk-shaped erythrocytes deformed to ellipsoidal disks under uniform shear flow [9] (Fig. 1a). The ratio short radius/long radius decreased with increasing shear stress: this ratio differed from one cell to another but was distributed in Gaussian function at a given shear stress, presumably due to the difference in their original size and deformability. The average of ratio could be used as a measure of deformability [10].

Upon calcium-loading, undeformable erythrocytes appeared distinctly (Fig. 1b and c). The

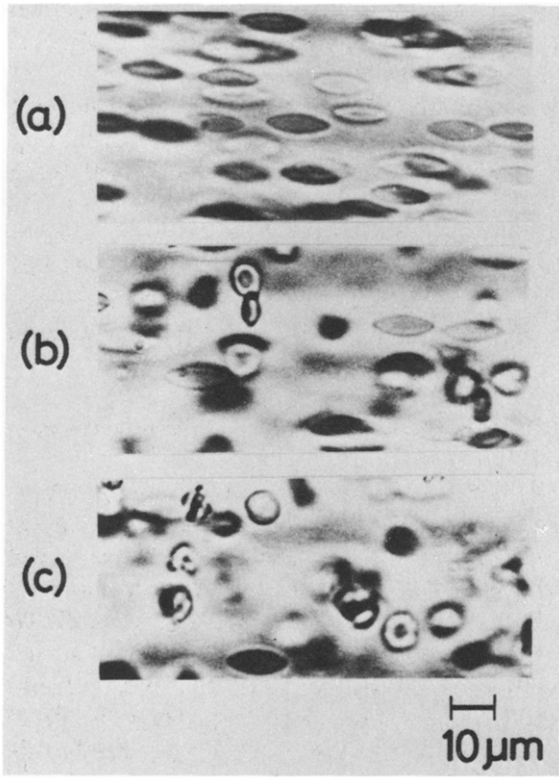

Fig. 1. Flash photographs of erythrocytes under uniform shear stress. The washed erythrocytes were incubated (a) without ionophore A23187 and $CaCl_2$, (b) with A23187 (1.5 μM) and $CaCl_2$ (4 μM), and (c) with ionophore A23187 (1.5 μM) and $CaCl_2$ (10 μM) for 40 min at 37°C. A uniform shear stress (140 dyn/cm^2) was applied using a rheoscope. The characteristics of these samples were as follows. (a) Calcium-unloaded erythrocytes, cell volume = 86.8 μm^3, $[Hb]_i$ = 36.4 g/dl, $[Ca]_i$ = 16.3 μmol/l packed cells = 1.41 amol per cell; all cells were deformed to ellipsoidal disk-shape, the ratio of short radius/long radius = 0.34 ± 0.03 (n = 67) at 140 dyn/cm^2 (25°C). (b) Calcium-loaded erythrocytes, cell volume = 76.3 μm^3, $[Hb]_i$ = 41.5 g/dl, $[Ca]_i$ = 44.6 μmol/l packed cells = 3.40 amol per cell; percentage of undeformable cells = 38%, the ratio of short radius/long radius of deformable cells = 0.36 ± 0.05 (n = 99), at 140 dyn/cm^2 (25°C). (c) Calcium-loaded erythrocytes, cell volume = 67.5 μm^3, $[Hb]_i$ = 49.5 g/dl, $[Ca]_i$ = 90.5 μmol/l packed cells = 6.11 amol per cell; percentage of undeformable cells = 83%, the ratio of short radius/long radius of deformable cells = 0.40 ± 0.05 (n = 32) at 140 dyn/cm^2 (25°C).

population of undeformable cells increased with increasing incubation time and concentrations of ionophore A23187 and $CaCl_2$, but the percentage became nearly constant after 40 min of incubation under our experimental conditions, thus the incubation time of 40 min was adopted throughout.

The population of undeformed cells increased with increasing calcium content (Fig. 2): under a shear stress of 140 dyn/cm^2, 50% of cells became undeformable at an intracellular calcium level of 40–50 μmol/l packed cells (= 3.5–4.0 amol/cell) and more than 90% of cells were undeformable above 100 μmol/l packed cells (= 6.5 amol/cell). On the other hand, the deformable cells in calcium-loaded samples showed a short radius/long radius ratio similar to that of calcium-unloaded cells, at corresponding shear stress.

The accumulation of calcium in the erythrocytes induced the reduction of the mean cell volume and the condensation of hemoglobin (Fig. 2), due to dehydration [2,3,4,19], but biconcavity was maintained in the present experimental conditions as judged from scanning electron microscopy (the incubation with more ionophore and $CaCl_2$ induced the transformation to echinocytes then to

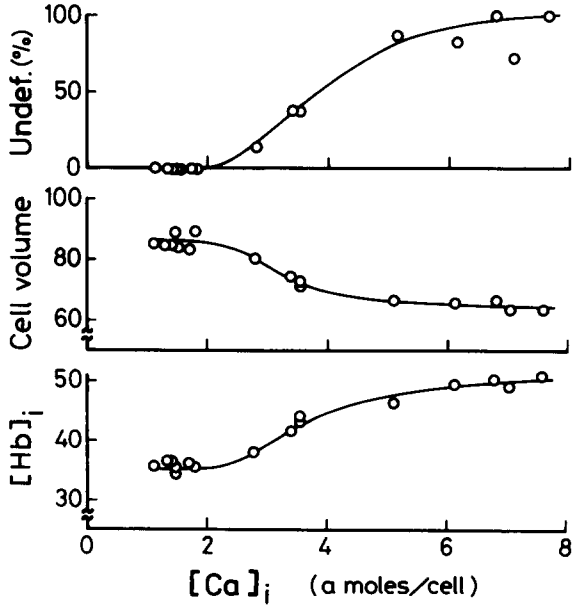

Fig. 2. Relationship between intracellular calcium content and percentage of undeformable cells, mean cell volume and hemoglobin concentration. The washed erythrocytes were incubated with or without ionophore A23187 (1.5 μM) and $CaCl_2$ (2–20 μM) in isotonic Hepes-saline solution containing glucose for 40 min at 37°C. The intracellular calcium contents were expressed in amol per cell. (Top) $[Ca]_i$ versus percentage of undeformable cells at 140 dyn/cm^2. (Middle) $[Ca]_i$ versus mean cell volume (μm^3). (Bottom) $[Ca]_i$ versus mean cell hemoglobin concentration (g/dl).

spherocytes, as is well known [2,20]). As seen in Fig. 2, a close relationship between percentage of undeformable cells and mean cell volume or mean cell hemoglobin concentration was evident.

Changes in membrane properties, induced by calcium-loading

The fluidity of lipid portion of the membrane was monitored by a spin label method: the motion of 16-SAL incorporated into erythrocyte membrane decreased upon calcium-loading. The temperature dependence of a spectral parameter, $\Delta W = [\Delta H_{pp}(0) \cdot (\sqrt{h(0)/h(1)} - 1)]$, is shown in Fig. 3, where $\Delta H_{pp}(0)$ is peak-to-peak line width of the central line, and $h(0)$ and $h(1)$ are the amplitudes of the central and low-field lines of the first derivative curve, respectively. This parameter is derived from the equation described in early literature [21] and increases as the motion of label molecule decreases. When the intracellular calcium content was augmented, the label motion decreased clearly, and also the disappearance of any

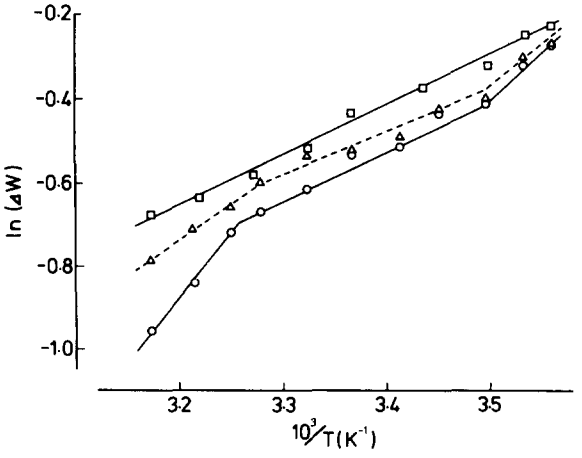

Fig. 3. Influence of intracellular calcium content on temperature dependence of the EPR parameter (ΔW of 16-SAL). The calcium-unloaded and -loaded erythrocytes (without/with A23187 and $CaCl_2$) were spin labeled with 16-SAL by the method described elsewhere [14]. The EPR parameter, ΔW, is defined in text. The properties of samples are as follows. (○), $[Ca]_i = 16.3$ μmol/l packed cells = 1.41 amol per cell; all cells were deformed to ellipsoidal disk-shape, the ratio of short radius/long radius = 0.34 ± 0.03 ($n = 67$) at 140 dyn/cm^2 (25°C). (△) $[Ca]_i = 47.4$ μmol/l packed cells = 3.53 amol per cell; percentage of undeformable cells = 38%, the ratio of deformable cells = 0.38 ± 0.04 ($n = 70$) at 140 dyn/cm^2 (25°C). (□), $[Ca]_i = 190$ μmol/l packed cells = 6.77 amol per cell; all cells were undeformable at 140 dyn/cm^2 (25°C).

distinct phase transition was noticed. Such decreased membrane fluidity was more evident at higher temperatures.

In addition, a slight decrease in mobility of 12-SAL in calcium-loaded erythrocyte membrane was detected: the order parameter [22] was 0.553 and 0.526 for the calcium-loaded (190 μmol/l packed cells) and unloaded cells at 38°C, respectively. In this connection, a crosslinking of membrane proteins could not be detected by SDS-polyacrylamide gel electrophoresis under the present experimental conditions.

Changes in energy metabolism, induced by calcium-loading

The decrease in ATP content during incubation with ionophore A23187 and $CaCl_2$ is well known [2,3,23]. As shown in Table I, ATP decreased, ADP and AMP increased, and the percentage of undeformable cells increased, when intracellular calcium content was augmented. The total adenylates slightly decreased, while the energy charge scarcely decreased at increasing calcium levels up to 100 μmol/l packed cells (= 6.5 amol/cell). When extensive calcium-loading was performed (Table I, last row), the energy charge decreased considerably and echinocytosis developed.

The amount of 2,3-diphosphoglycerate did not change in the present experimental conditions, but it decreased gradually by extensive calcium-loading: e.g., approx. 10% decrease was observed by incubation with 5 μM A23187 and 50 μM $CaCl_2$ for 60 min at 37°C.

Influence of cell volume changes on deformability

In order to see the influences of intracellular hemoglobin concentration on the cellular deformability, erythrocytes (either calcium-loaded or unloaded) were exposed to media of different osmolarity for 30 min at 37°C. Then the deformability was measured in 20% (w/v) Dextran T-40 of corresponding osmolarity (Fig. 4a). When calcium-loaded cells were exposed to hypotonic media, the mean cell volume increased and the percentage of undeformable cells decreased, i.e., some undeformable cells became deformable by osmotic swelling. On the other hand, when calcium-unloaded cells were exposed to hypertonic media, undeformable cells were produced by

TABLE I

INFLUENCE OF CALCIUM-LOADING ON WHOLE ERYTHROCYTES

The washed erythrocytes were incubated with ionophore A23187 and $CaCl_2$ (concentrations given in the table) for 40 min at 37°C. The sample shown in last row (case E) was calcium overloaded and transformed to echinocytes, otherwise the erythrocytes maintained their biconcave disk-shape.

	Incubation with		$[Ca]_i$[a]		Cell[b] volume (μm^3)	$[Hb]_i$[c] (g/dl)	[ATP]	[ADP]	[AMP]	Total[d]	EC[e]	G6PDH[f]	Undeform.[g] cells (%)		Ratio[h]	
	A23187 (μM)	$CaCl_2$ (μM)	μM	amol/cell			(amol/cell						(14)	(140)	(14)	(140)
A	0	0	15.4	1.34	86.8	36.5	103.0	22.7	1.8	127.0	0.90	159	6	0	0.76	0.36
B	1.5	2	26.3	1.97	74.9	43.0	81.8	29.4	2.6	113.0	0.85	170	47	46	0.74	0.36
C	1.5	4	47.6	3.53	74.2	44.0	69.5	26.6	3.1	99.2	0.84	159	63	60	0.72	0.37
D	1.5	10	90.5	6.11	67.5	49.4	50.1	34.5	11.0	95.6	0.71	164	84	83	0.77	0.38
E[i]	3.0	25	118	7.65	64.8	50.9	41.6	33.2	24.1	98.9	0.59	–	100	100	–	–

[a] $[Ca]_i$ expressed by μmol/l packed cells and amol per cell.
[b] Mean cell volume.
[c] Mean cell hemoglobin concentration.
[d] Total adenylates = [ATP]+[ADP]+[AMP].
[e] Energy charge = (2[ATP]+[ADP])/2([ATP]+[ADP]+[AMP]).
[f] Glucose-6-phosphate dehydrogenase activity (units/10^{12} cells), measured at 24°C.
[g] Population of undeformable cells (%), at shear stress shown in parentheses (dyn/cm^2) at 25°C.
[h] Mean ratio of short radius/long radius of deformed cells at shear stress shown in parentheses (dyn/cm^2) at 25°C.
[i] Examples of overloaded calcium: all erythrocytes transformed to echinocytes.

osmotic shrinking. However, the deformability of calcium-loaded cells in hypotonic media was not perfectly restored, e.g., calcium-loaded cells in 150 mosM solution contained more undeformable cells than calcium-unloaded cells in 350 mosM solution, in spite of the same mean cell hemoglobin concentration (Fig. 4b).

Fractionation of deformable and undeformable cells, after calcium-loading

The calcium-loaded erythrocytes, containing both deformable and undeformable cells, were fractionated by density gradient centrifugation using Percoll. The low-density cells (separated as light fraction) were larger and more deformable than that of deformable cells before fractionation. On the other hand, the high-density cells (in heavy fraction) were smaller in volume and did not deform, even at 140 dyn/cm^2 (Table II). The high-density cells contained less ATP and showed lower glucose-6-phosphate dehydrogenase activity, compared with the low density cells. Since the enzyme activity is known to be low in aged cells [24–26], the high density, undeformable cells were aged cells and the low density, deformable cells were younger cells. Presumably, the preferential calcium-loading into aged erythrocytes leads to the dehydration and the loss of deformability of these cells.

Cell age-dependent difference in deformability and calcium accumulation

The low density and high density cells were fractionated from the fresh erythrocytes using Percoll [11], then washed and incubated with ionophore A23187 and $CaCl_2$. The results are summarized in Table III and Fig. 5.

(a) Before calcium-loading, the light fraction

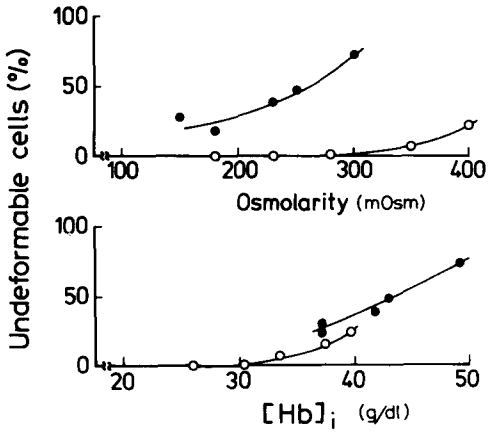

Fig. 4. Influence of osmotic volume changes on percentage of undeformable erythrocytes, comparison of calcium-unloaded and -loaded cells. The erythrocytes, either calcium-unloaded and -loaded, were further incubated in various osmolar solution for 30 min at 37°C. (Top) Osmolarity of media (mosM) versus percentage of undeformable cells. (Bottom) Mean cell hemoglobin concentration (g/dl) in various osmolar solutions versus percentage of undeformable cells at 140 dyn/cm^2 (25°C). Properties of erythrocytes in 285 mosM solution were as follows. (○), calcium-unloaded erythrocytes; cell volume = 87.1 μm^3, [Hb]$_i$ = 35.3 g/dl, [Ca]$_i$ = 18.2 μmol/l packed cells = 1.58 amol per cell. (●), calcium-loaded erythrocytes; cell volume = 65.4 μm^3, [Hb]$_i$ = 49.1 g/dl, [Ca]$_i$ = 107.4 μmol/l packed cells = 7.02 amol per cell.

TABLE II

PROPERTIES OF DENSITY FRACTIONATED ERYTHROCYTES, AFTER CALCIUM-LOADING

The washed erythrocytes were incubated with A23187 (1.5 μM) and $CaCl_2$ (4 μM) for 40 min at 37°C. After removal of ionophore A23187 and $CaCl_2$, the cells were fractionated by density gradient centrifugation using Percoll. For footnotes a–h see Table I.

	[Ca]$_i$ [a]		Cell [b] volume (μm^3)	[Hb]$_i$ [c] (g/dl)	[ATP]	[ADP]	[AMP]	Total [d]	EC [e]	G6PDH [f]	Undeform. [g] cells (%)		Ratio [h]	
	μM	amol/cell			(amol per cell)						(14)	(140)	(14)	(140)
Before incubation	16.3	1.31	85.7	37.3	112.0	17.3	1.7	131.0	0.92	154	5	0	0.75	0.35
After calcium-loading	46.0	3.60	77.2	41.5	–	–	–	–	–	–	36	30	0.76	0.34
Light fraction [i] (13.4%)	–	–	93.9	34.3	94.9	30.4	2.5	127.8	0.86	187	0	0	0.70	0.34
Heavy fraction [i] (23.5%)	–	–	65.9	44.1	80.9	15.8	2.3	99.0	0.90	89	100	100	–	–

[i] Percent fraction to total erythrocytes, on the basis of hemoglobin concentration, is given in parenthesis.

TABLE III

INFLUENCE OF CALCIUM-LOADING TO FRACTIONATED ERYTHROCYTES (YOUNGER AND AGED CELL FRACTIONS)

The fresh erythrocytes were fractionated by density gradient centrifugation using Percoll. Both light fraction (rich in younger cells) and heavy fraction (rich in aged cells) were incubated with A23187 (1.5 μM) and $CaCl_2$ (10 μM) for 40 min at 37°C. For footnotes a–e see Table I.

	$[Ca]_i$ [a]		Cell [b] volume (μm^3)	$[Hb]_i$ [c] (g/dl)	[ATP]	[ADP]	[AMP]	Total [d]	EC [e]	G6PDH [f]	Undeform. [g] cells (%)		Ratio [h]	
	μM	amol/cell			(amol per cell)						(14)	(140)	(14)	(140)
Before fraction	17.1	1.54	90.3	34.6	99.6	11.1	1.3	112.0	0.94	171	3	0	0.74	0.33
Light fraction [i] (10.1%)														
before calcium-load	14.5	1.39	96.1	31.6	99.2	19.8	1.7	120.7	0.90	246	3	0	0.69	0.30
after calcium-load	21.0	1.92	91.2	33.7	96.1	17.3	1.5	114.9	0.91	261	11	3	0.68	0.31
Heavy fraction [i] (15.0%)														
before calcium-load	32.7	2.85	87.2	37.3	77.9	18.8	2.2	98.6	0.88	151	9	2	0.79	0.36
after calcium-load	48.7	3.75	76.9	42.4	79.2	16.1	2.2	97.5	0.90	154	61	35	0.75	0.35

[f] Glucose-6-phosphate dehydrogenase activity (units/10^{12} cells), measured at 28°C.

[g] Population of undeformable cells (%), at shear stress shown in parentheses (dyn/cm^2) at 25°C.

[h] Mean ratio of short radius/long radius of deformed cells at shear stress shown in parentheses (dyn/cm^2). The difference in ratios between light and heavy fractions, both before and after calcium-loading, is statistically significant (by t-test, $p < 0.005$) at 14 and 140 dyn/cm^2.

[i] Percent fraction to total erythrocytes, on the basis of hemoglobin concentration, is given in parenthesis.

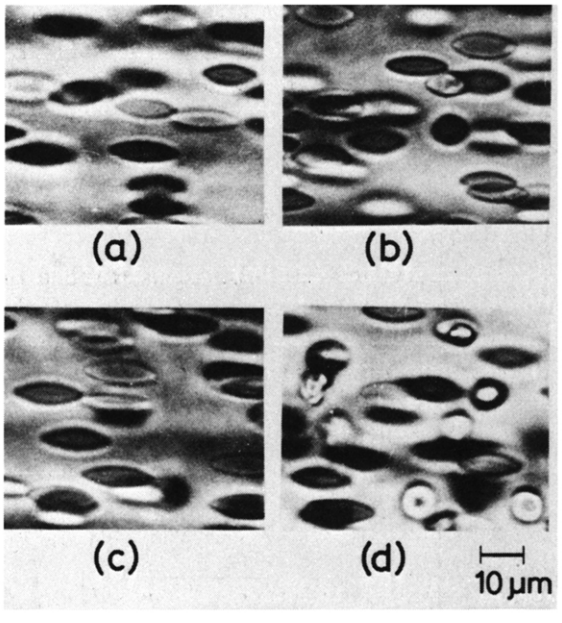

Fig. 5. Flash photographs of younger and aged erythrocytes, before and after calcium-loading, under uniform shear stress. The fresh erythrocytes were fractionated by density gradient centrifugation using Percoll to heavy and light fractions. They were then incubated with ionophore A23187 (1.5 μM) and $CaCl_2$ (10 μM) for 40 min at 37°C. A uniform shear stress (140 dyn/cm^2) was applied using a rheoscope. (Left) Light fraction, rich in younger cells; (right) heavy fraction, rich in aged cells. (Top) Before calcium-loading, (bottom) after calcium-loading. The properties of the cells are summarized in Table III.

consisted mostly of younger cells, having larger cell volume, containing more ATP and less calcium and showing higher activity of glucose-6-phosphate dehydrogenase: in contrast, the heavy fraction was rich in aged cells, which were of smaller volume, contained less ATP and more calcium and showed lower dehydrogenase activity. The younger cells were more deformable than the aged cells, as judged from the ratio of short radius/long radius under shear stress.

(b) After incubation with ionophore A23187 and $CaCl_2$, the intracellular calcium level of younger (low density) cells increased, there was a slight decrease of cell volume but no change in ATP content and in deformability. On the other hand, the calcium accumulation in aged (high density) cells produced complete loss of deformability and marked dehydration without loss of ATP. In

all cases the energy charge scarcely altered; therefore the utilization and regeneration of ATP was balanced during the calcium-loading, though the amount of adenylates in aged cells was originally less than that in younger cells.

Discussion

Causes of diminished deformability in calcium-loaded erythrocytes

It has long been known that (i) calcium-loading to erythrocytes in low-K^+ media induces loss of intracellular K^+ and water [4,27], and (ii) the (sphero)echinocytes induced by extensive calcium-loading are undeformable and their membrane proteins are crosslinked [28]. However, in the present study, mild calcium-loading up to 100 μmol/l packed cells did not induce complete ATP depletion, echinocytosis and protein crosslinking, although decreased cell volume and condensed hemoglobin became evident as the calcium level was augmented.

Upon increasing the intracellular calcium content, a distinct transition of erythrocytes from the deformable to the undeformable state was observed, while biconcavity was maintained (Figs. 1 and 2). Quantitatively, 50% transition occurred at 2–3-times the normal calcium level, and more than 90% transition to undeformable state occurred at 4–5-times the normal level. The increase in number of undeformable cells also paralleled the decrease in cell volume (thus, the increased intracellular hemoglobin concentration). On the other hand, the deformability of deformable cells to ellipsoidal disk under uniform shear stress (14–140 dyn/cm^2) was unaltered at any calcium level tested. A gradual decrease in erythrocyte filtrability caused by a slight increase in calcium content (up to 20%) has been reported [29]. The discrepancy may arise from the difference of the method used: the photographic observation by rheoscopy can easily differentiate deformable and undeformable cells in shear flow, but the filtration method cannot differentiate such individual deformation (thus an addition of hardened cells to intact cells affects the filtrability, as observed for calcium-loaded cells).

Factors determining the cellular deformability are: (i) cell shape or surface/volume ratio; (ii) internal viscosity or intracellular hemoglobin concentration; and (iii) flexibility of cell membrane [5]. In order to explain deformability of calcium-loaded erythrocytes, the contribution of all factors should be considered: (i) mean cell volume decreased (Fig. 2) and flattening of cells occurred, though the biconcave shape was maintained; (ii) the mean cell hemoglobin concentration increased (Fig. 2); and (iii) a decrease in lipid membrane fluidity was detected by the spin-label method (Fig. 3) without crosslinking of membrane proteins.

Calcium-loaded cells exposed to hypotonic media always contained more undeformable cells than the unloaded cells exposed to hypertonic media, in spite of the same mean cell hemoglobin concentration (Fig. 4). These observations suggest a calcium-induced alteration of membrane organization towards loss of deformability. Therefore, (i) the main reason for the complete loss of deformability in calcium-loaded erythrocytes seemed to be the increased internal viscosity (condensation of hemoglobin), as already proposed for ATP-depleted and calcium-loaded erythrocytes [4]; however, (ii) the alteration in membrane mechanical properties due to calcium accumulation could not be ignored in this case, since many studies on erythrocyte ghosts show the contribution of intracellular Ca^{2+}, Mg^{2+} and ATP to the membrane organization [30–33].

Balance between energy metabolism and calcium accumulation

Ca^{2+} entering into erythrocytes is extruded by the Ca^{2+}-pump at the expense of ATP, and the activity of the Ca^{2+}-pump is regulated by Ca^{2+}-calmodulin [6,7]. Furthermore, Ca^{2+} itself or Ca^{2+}-calmodulin modifies K^+-permeability [34,35] and Na^+-permeability [36], as well as the activity of many enzymes. Therefore, as calcium-loading progresses, the requirement for ATP increases and the balance of energy metabolism must be affected.

The present results (Figs. 1 and 2, Table I) show a close relation between increased calcium content, decreased ATP, decreased volume and percentage of undeformable cells. Between these phenomena and the ability of erythrocytes to extrude Ca^{2+} a connection might exist as follows:

during calcium-loading procedure, the high energy charge (0.84–0.95) was maintained against calcium accumulation up to 3–4-times of normal erythrocytes in average (approx. 50–60 μmol/l packed cells), i.e., ATP regeneration could be balanced to energy requirement in spite of calcium accumulation. However, when the intracellular calcium content reached more than 5-times the normal level (approx. 100 μmol/l packed cells), the ATP regeneration could not meet the ATP requirement and the energy charge sharply fell off.

Relation between calcium accumulation and cell age

As shown in Table II, the undeformable and deformable cells after calcium-loading were distinctly fractionated by the density gradient centrifugation. The former, of high density, were aged cells, while the latter, of low density, were younger cells, as judged from the activity of glucose-6-phosphate dehydrogenase [24–26] (the activity was not altered by the calcium-loading procedure as seen in Table I).

The density gradient centrifugation with Percoll fractionated aged cells from fresh erythrocytes, as judged from biochemical and rheological properties (Table III). The decreased deformability of aged cells (Table III and Fig. 5) is complex [37,38], since (i) the decreased surface/volume ratio due to loss of membrane components [39,40], (ii) the increased internal viscosity due to the condensation of hemoglobin (Table III), and (iii) the alteration of membrane organization detected by the decreased fluidity of membrane lipids [41,42] all contribute to it. Furthermore, in aged cells, the increased calcium and the decreased ATP content (Table III) [38,39,41,43], the change in calcium distribution inside the cells [44], the decreased Mg^{2+} level [43,45], the decreased calmodulin activity [46,47], and so forth, may modify the cytoskeletal conformation and lead to changes in viscoelasticity of the membrane [48].

Upon calcium-loading, the younger cells complied well to shear stress in spite of increased calcium content (38%, in Table III), while many aged cells became undeformable, owing to increased calcium content (32%), decreased volume (12%) and increased hemoglobin concentration (14%) occurring without change in ATP level.

Surveying these results, it is certain that (i) the younger cells resist calcium-loading with A23187 and $CaCl_2$, as judged from the maintenance of cell volume and deformability, in spite of increased calcium content; (ii) the aged cells (originally less deformable and with more calcium) become undeformable upon calcium-loading, because of increased internal viscosity (caused by loss of K^+ and water); (iii) upon extensive calcium-loading (Table I, case D), most erythrocytes except for younger cells become undeformable, decreased in energy charge and reduced in cell volume. Therefore, the progressive appearance of undeformable cells induced by calcium-loading (Fig. 2 and Table I) seems to be caused by the preferential accumulation of calcium into those cells having low energy metabolism.

Change of membrane fluidity by calcium-loading, in relation to deformability

In the present study using a fatty acid spin label (16-SAL), the decreased acyl chain motion at the middle portion of lipid bilayer was clearly detected at a calcium level of less than 100 μmol/l packed cells, without cross-linking of membrane proteins.

The decreased lipid membrane fluidity induced by calcium accumulation (Fig. 3) may be explained in terms of (i) the structural changes of spectrin network: possibly due to alteration in calmodulin-spectrin binding [49], modified cross-linking of the spectrin-actin-band 4.1 [50], stimulated membrane protein phosphorylation [51] and Ca^{2+}-spectrin interaction [52,53] and (ii) altered lipid bilayer organization: due to preferential binding of Ca^{2+} with phosphatidylserine and complex interaction among Ca^{2+}, phospholipids and spectrin [55–57]. The present result with spin label shows clearly the Ca^{2+}-induced modification of membrane organization, but the reason for it and its relevance to the deformability still remain unclear.

Acknowledgement

This work was supported by grant from Ministry of Education, Culture and Science of Japan.

References

1 Weed, R.I., LaCelle, P.L. and Merrill, E.W. (1969) J. Clin. Invest. 48, 795–809

2 Kirkpatrick, F.H., Hillman, D.G. and LaCelle, P.L. (1975) Experientia 31, 653–654
3 Dreher, K.L., Eaton, J.W., Breslawec, K., Berger E., Blackshear, P.L. and White, J.G. (1980) Am. J. Pathol. 101, 543–555
4 Clark, M.R., Mohandas, N., Feo, C., Jacobs, M.S. and Shohet, S.B. (1981) J. Clin. Invest. 67, 531–539
5 Chien, S. (1975) in The Red Blood Cells, 2nd Edn. (Surgenor, D.M., ed.), Vol. 2, pp. 1031–1133, Academic Press, New York
6 Vincenzi, F.F. and Hinds, T.R. (1980) in Calcium and Cell Function (Cheung, W.Y., ed.), Vol. 1, pp. 127–165, Academic Press, New York
7 Schatzmann, H.J. (1983) Annu. Rev. Physiol. 45, 303–312
8 O'Rear, E.A., Udden, M.M., McIntire, L.V. and Lynch, E.C. (1981) Am. J. hematol. 11, 283–292
9 Schmid-Schönbein, H. and Wells, R. (1969) Science 165, 288–291
10 Maeda, N., Kon, K., Imaizumi, K., Sekiya, M. and Shiga, T. (1983) Biochim. Biophys. Acta 735, 104–112
11 Pertoft, H., Laurent, T.C., Låås, T. and Kågedal, L. (1978) Anal. Biochem. 88, 271–282
12 Van Kampen, E.J. and Zijlstra, W.G. (1970) Clin. Chim. Acta 6, 538–544
13 Suda, T., Maeda, N., Shimizu, D., Kamitsubo, E. and Shiga, T. (1982) Biorheology 19, 555–565
14 Shiga, T., Suda, T. and Maeda, N. (1977) Biochim. Biophys. Acta 466, 231–244
15 Fairbanks, G., Steck, T.L. and Wallach, D.F.H. (1971) Biochemistry 10, 2606–2617
16 Maeda, N., Kon, K., Sekiya, M. and Shiga, T. (1980) Br. J. Haematol. 45, 467–480
17 Maeda, N., Chang, H., Benesch, R. and Benesch, R.E. (1971) New Engl. J. Med. 284, 1239–1241
18 Löhr, G.W. and Waller, H.D. (1974) in Methods of Enzymatic Analysis (Bergmeyer, H.U., ed.), 2nd Edn., Vol. 2, pp. 636–641, Verlag Chemie, Weinheim
19 Lake, W., Rasmussen, H. and Goodman, D.B.P. (1977) J. Membrane Biol. 32, 93–113
20 White, J.G. (1976) Semin. Hematol. 13, 121–132
21 Stone, T.J., Buckman, T., Nordio, P.L. and McConnell, H.M. (1965) Proc. Natl. Acad. Sci. USA 54, 1010–1017
22 Hubbell, W.L. and McConnell, H.M. (1969) Proc. Natl. Acad. Sci. USA 64, 20–27
23 Plishker, G.A. and Gitelman, H.J. (1977) J. Membrane Biol. 35, 309–318
24 Sass, M.D., Vorsanger, E. and Spear, P.W. (1964) Clin. Chim. Acta 10, 21–26
25 Brok, F., Ramot, B., Zwang, E. and Danon, D. (1966) Isr. J. Med. Sci. 2, 291–296
26 Fornaini, G., Dacha, M., Fazi, A., Gargano, M. and Schiavo, E. (1969) Eur. J. Biochem. 7, 214–222
27 Gardos, G. (1958) Biochim. Biophys. Acta 30, 653–654
28 Smith, B.D., LaCelle, P.L., Siefring, G.E., Lowe-Krentz, L. and Lorand, L. (1981) J. Membrane Biol. 61, 75–80
29 O'Rear, E.A., Udden, M.M., McIntire, L.V. and Lynch, E.C. (1982) Biochim. Biophys. Acta 691, 274–280
30 Palek, J., Curby, W.A. and Lionetti, F.J. (1971) Am. J. Physiol. 220, 19–26
31 Quist, E.E. and Roufogalis, B.D. (1976) Biochem. Biophys. Res. Commun. 72, 673–679
32 Quist, E.E. (1980) Arch. Biochem. Biophys. 203, 123–133
33 Jimbu, Y., Sato, S. and Nakao, M. (1984) Nature 307, 376–377
34 Schwarz, W. and Passaw, H. (1983) Annu. Rev. Physiol. 45, 359–374
35 Grygorczyk, R., Schwarz, W. and Passaw, H. (1984) Biophys. J. 45, 693–698
36 Brown, A.M. and Lew, V.C. (1983) J. Physiol. (Lond.) 343, 455–493
37 Shiga, T. and Maeda, N. (1980) Biorheology 17, 485–499
38 Nash, G.B. and Meiselman, H.J. (1981) Microcirculation 1, 255–284
39 Cohen, N.S., Ekholm, J.E., Luthra, M.G. and Hanahan, D.J. (1976) Biochim. Biophys. Acta 419, 229–242
40 Seaman, G.V.F., Knox, R.J., Nordt, F.J. and Regan, D.H. (1977) Blood 50, 1001–1010
41 Shiga, T., Maeda, N., Suda, T., Kon, K. and Sekiya, M. (1979) Biochim. Biophys. Acta 553, 84–95
42 Bartosz, G. (1981) Biochim. Biophys. Acta 664, 69–73
43 LaCelle, P.L., Kirkpatrick, F.H., Udkow, M.P. and Arkin, B. (1972) Nouv. Rev. Franç. Hématol. 12, 789–798
44 Schrier, S.J., Johonson, M., Junga, I. and Krueger, J. (1980) Blood 56, 667–678
45 Watson, W.S., Lyon, T.D.B. and Hilditch, T.E. (1980) Metabolism 29, 397–399
46 Ekholm, J.E., Shukla, S.D. and Hanahan, D.J. (1981) Biochem. Biophys. Res. Commun. 103, 407–413
47 Monzon, C.M., Penniston, J.T., Fairbanks, V.F. and Burgert, E.O. (1982) Br. J. Haematol. 51, 261–264
48 Nash, G.B. and Meiselman, H.J. (1983) Biophys. J. 43, 63–73
49 Sobue, K., Muramoto, Y., Fujita, M. and Kakiuchi, S. (1981) Biochem. Biophys. Res. Commun. 100, 1063–1070
50 Foeler, V. and Taylor, L .(1980) J. Cell. Biol. 85, 361–376
51 Nelson, M.J., Daleke, D.L. and Huestis, W.H. (1982) Biochim. Biophys. Acta 686, 182–188
52 Cassoly, R., Daveloose, D., Wolf, C. and Leterrier, F. (1978) Compt. Rend. Acad. Sci. (Paris) 286, 1009–1012
53 Lamel, B. and Maier, G. (1980) Biochim. Biophys. Acta 622, 245–258
54 Ohnishi, S. and Ito, T. (1973) Biochem. Biophys. Res. Commun. 51, 132–138
55 Van Dijck, P.W.M., De Kruijff, B., Verkleij, A.J., Van Deenen, L.L.M. and De Gier, J. (1978) Biochim. Biophys. Acta 512, 84–96
56 Mombers, C., De Gier, J., Demel, R.A. and Van Deenen, L.L.M. (1980) Biochim. Biophys. Acta 603, 52–62
57 Yamada, S. and Ohnishi, S. (1983) Acta Haematol. Jap. 46, 1406–1413